The Astrophysical Journal, 922:100 (9pp), 2021 December 1 https://doi.org/10.3847/1538-4357/ac2fa3

Theoretical Study of the Rotational Structure of the $c_4'^1\Sigma_u^+$ (6)–$X^1\Sigma_g^+$(0–9) Absorption Bands of N_2

A. M. Velasco, J. L. Alonso, P. Redondo, and C. Lavín
Departamento de Química Física y Química Inorgánica, Facultad de Ciencias, Universidad de Valladolid, E-47005 Valladolid, Spain; clavin@qf.uva.es
Received 2021 June 16; revised 2021 October 8; accepted 2021 October 9; published 2021 November 24

Abstract

We have theoretically determined the absorption oscillator strengths and wavenumbers for rotationally resolved transitions of the $c_4'^1\Sigma_u^+$ (6)-$X^1\Sigma_g^+$(0–9) bands of N_2, which are relevant to analyze the spectra of planetary atmospheres. The Molecular Quantum Defect Orbital method has been used in our calculations. The interaction between the $c_4'^1\Sigma_u^+$ (6) Rydberg state and the $b'^1\Sigma_u^+$ valence states has been considered using an adequate rovibronic energy matrix. In addition, we have calculated the lifetimes of the rotational levels of the $c_4'^1\Sigma_u^+$ (6) state. We hope that the reported data, most of them for the first time, can be useful in the interpretation of planetary atmospheres where N_2 is present.

Unified Astronomy Thesaurus concepts: Molecular spectroscopy (2095); Line intensities (2084); Radiative processes (2055)

1. Introduction

The $c_4'^1\Sigma_u^+$-$X^1\Sigma_g^+$ Rydberg band system of molecular nitrogen, also named the Carroll–Yoshino bands, plays an essential role in the interpretation of extreme ultraviolet (EUV) emission observations in the airglow upper atmosphere of the Earth and other nitrogen-rich planetary atmospheres. Several bands of the $c_4'^1\Sigma_u^+$(0, 3, 4, 6)-$X^1\Sigma_g^+$(v″) progressions have been observed in Earth's airglow spectra (Feldman et al. 2001) obtained with the Far Ultraviolet Spectroscopic Explorer (FUSE) and in the EUV spectrum of Titan's atmosphere (Ajello et al. 2007; Stevens et al. 2011) achieved using the Ultraviolet Imaging Spectrometer (UVIS) on Cassini. Most of the research so far has been focused on the $c_4'^1\Sigma_u^+$(0, 3, 4)-$X^1\Sigma_g^+$(v″) progressions (see, for example, Ajello et al. 1998; Walter et al. 2000; Liu et al. 2008). The $c_4'^1\Sigma_u^+$ (6)-$X^1\Sigma_g^+$(v″) bands have been investigated less frequently, despite their observation in spectra from atmospheres dominated by molecular nitrogen. Feldman et al. (2001) identified the $c_4'^1\Sigma_u^+$ (6)-$X^1\Sigma_g^+$(4, 5, 8) bands in the terrestrial airglow spectra obtained with FUSE. These bands, together with the $c_4'^1\Sigma_u^+$ (6)-$X^1\Sigma_g^+$(7) band, have been observed in the EUV spectra of Titan's atmosphere obtained by UVIS (Ajello et al. 2007; Stevens et al. 2011). The $c_4'^1\Sigma_u^+$ (6)-$X^1\Sigma_g^+$(8) band has also been observed in the spectrum of Mars, obtained with FUSE (Krasnopolsky & Feldman 2002). As claimed by Stark et al. (2005) and Liu et al. (2009), the quantitative interpretation of the observations in such atmospheres and the modeling of the upper atmospheric processes require reliable spectroscopic data, including line positions, oscillator strengths, and lifetimes with rotational effects.

Several studies have been performed on the $c_4'^1\Sigma_u^+$ (6)-$X^1\Sigma_g^+$(v″) progression at band level. The $c_4'^1\Sigma_u^+$ (6)-$X^1\Sigma_g^+$(1–9) bands were observed in the vacuum ultraviolet (VUV) emission spectrum of molecular nitrogen (Roncin et al. 1987). Emission cross-sections for v″ progression from the $c_4'^1\Sigma_u^+$ (6) state were measured at medium—(Ajello et al. 1989) and high-resolution (Heays et al. 2014). The band oscillator strength, or *f* -value, for the $c_4'^1\Sigma_u^+$ (6)-$X^1\Sigma_g^+$(v″=0) was derived from experimental measurements (Zipf & McLaughlin 1978; Ajello et al. 1989; Chan et al. 1993; Huber et al. 2009; Heays 2010). Calculations of oscillator strengths for the $c_4'^1\Sigma_u^+$ (6)-$X^1\Sigma_g^+$(0–12) bands were reported by Lavín & Velasco (2016). The fluorescence lifetime of the $c_4'^1\Sigma_u^+$ (6) state was measured by Moise et al. (2011). At the rotational level, energies for the rovibronic levels of the $c_4'^1\Sigma_u^+$ (6) and rotational lines of the $c_4'^1\Sigma_u^+$ (6)-$X^1\Sigma_g^+$(v″) progression were measured by Roncin et al. (1998).

To achieve a better understanding of planetary observations, where the $c_4'^1\Sigma_u^+$ (6)-$X^1\Sigma_g^+$(v″) bands of N_2 are present, in this work, we have calculated transition energies and line intensities, expressed as oscillator strengths or *f*-values, for *R* and *P* branches of the $c_4'^1\Sigma_u^+$ (6)-$X^1\Sigma_g^+$(0–9) bands. It is well known that the vibrational levels of the $c_4'^1\Sigma_u^+$ Rydberg state of N_2 interact with the appropriate vibrational levels of the $b'^1\Sigma_u^+$ valence state (Yoshino et al. 1979; Stahel et al. 1983). Hence, in our calculations, we have taken into account this homogeneous perturbation between states of $^1\Sigma_u^+$ symmetry through an interaction matrix for each value of the rotational quantum number *J*. The description of the $c_4'^1\Sigma_u^+$ Rydberg state has been made with the molecular quantum defect orbital (MQDO) method, which has proven to be a reliable approach in dealing with rovibronic transitions of N_2 in earlier applications (Lavín et al. 2008, 2010; Lavín & Velasco 2011; Velasco & Lavín 2020). We have also determined the radiative lifetimes of the rotational levels of the $c_4'^1\Sigma_u^+$ (6) state, which can be helpful to elucidate the competition between predissociation and radiation in N_2 emissions.

2. Method of Calculation

In a diatomic molecule, the dimensionless absorption oscillator strength for a rotational line can be defined in the following form (Larsson 1983):

$$f_{v'J',v''J''} = \frac{8\pi^2 mca_0^2}{3h}\nu_{v'J',v''J''}\frac{S_{J'J''}}{2J''+1}, \quad (1)$$

where $\nu_{v'J',v''J''}$ are the line wavenumbers in cm^{-1} and $S_{J'J''}$ is the rotational line strength in atomic units. Primed quantities refer to the upper electronic state and double primes designate the lower state. This standard notation is used throughout the paper.

The wave function for a diatomic molecule can be separated into independent electronic and nuclear factors, and the nuclear term can be approximated to the product of the rotational and vibrational wave functions. Then, the rotational line strength can be written as the multiplication of independent vibrational, electronic, and rotational factors (Whiting & Nicholls 1974) in the following way:

$$S_{J'J''} = q_{v'v''} R_e^2 \Im_{J'J''}, \quad (2)$$

where $q_{v'v''}$ is the Franck–Condon factor, R_e is the electronic transition moment expressed in atomic units, and $\Im_{J'J''}$ is the Hönl–London factor.

The factorization of Equation (2) is no longer appropriate when rotational perturbation happens. In this case, interactions between the rotational excitation states should be considered to adequately describe the rovibronic structure of the absorption spectra. To this end, each perturbed electronic state of a rovibrational level should be characterized by an appropriate linear combination of diabatic unperturbed basis states (Walter et al. 2000). Therefore, the expression for the line strength is transformed as follows:

$$S_{J'J''} = \left| \sum_k C_k \langle v'_k | v'' \rangle R_e^k (\Im_{J'J''})^{1/2} \right|^2, \quad (3)$$

where C_k is the coefficient of the k_{th} basis state, $\langle v'_k | v'' \rangle$ is the vibrational overlap integral, and R_e^k is the electronic moment between the lower electronic state and the upper k_{th} diabatic state. The overlap integrals were determined using vibrational wave functions obtained by solving the Schödinger equation with the Numerov algorithm from potential energy curves calculated with a Rydberg–Klein–Rees (RKR) approach (Rydberg 1931; Klein 1932; Rees 1947).

Ck's perturbation components have been obtained by diagonalization of an interaction matrix for each J value. The diagonal and off-diagonal elements are the unperturbed rotational energies of the states and the interaction parameters, respectively. The Hönl–London factors have been estimated following the equations reported by Kovács (1969). The electronic transition moment of the transitions involving the Rydberg states has been determined with the MQDO method.

The MQDO methodology was formulated to deal with molecular Rydberg transitions and has been described in detail in previous papers (Martín et al. 1996). In this approach, the radial part of the wave functions is the analytical solution of a one-electron Schrödinger equation containing a model potential. On the other hand, the angular part of the molecular Rydberg wave functions is a symmetry-adapted linear combination of spherical harmonics. In such a way, the transition moment for a transition between two unperturbed electronic states i and j is expressed as the product of a radial and angular contribution:

$$R_e^2 = Q\{i \rightarrow j\} R_{ij}(r)^2, \quad (4)$$

where $Q\{i \rightarrow j\}$ is the angular factor that results from the integration of the angular part of the MQDOs and that of the transition dipole moment operator, and $R_{ij}(r)$ is the radial part of the electronic transition moment. One of the advantages of the MQDO approach is that the transition integrals result in closed-form analytical expressions, which avoids numerical errors and convergence problems.

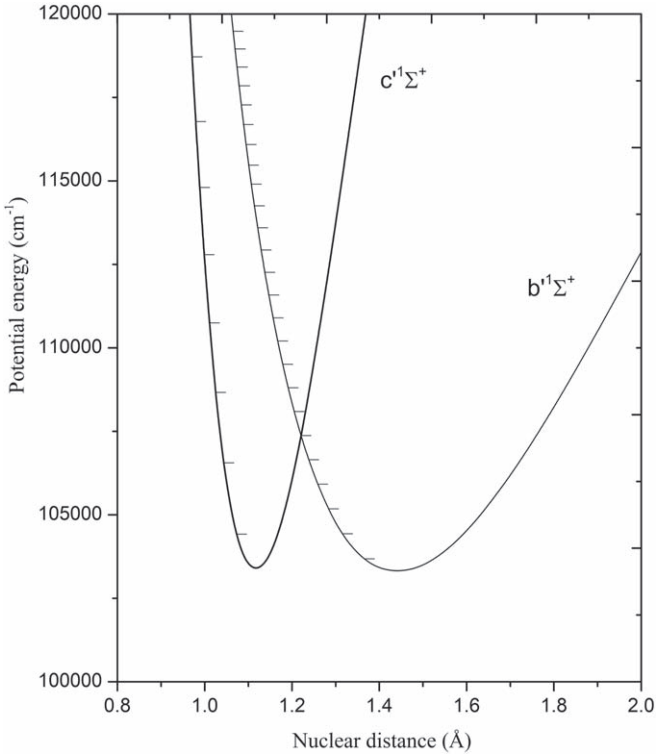

Figure 1. Potential energy curves for the diabatic $c_4'^1\Sigma_u^+$ and $b'^1\Sigma_u^+$ states of N_2.

3. Results and Discussion

The $c_4'^1\Sigma_u^+$ (6)-$X^1\Sigma_g^+$(0–9) bands are the result of rovibronic absorption transitions from the $v'' = 0$–9 vibrational levels of the ground state $X^1\Sigma_g^+$ to the $\acute{v} = 6$ vibrational level of the lowest member of the Rydberg $np\sigma$ series (with $n = 3$). Stahel et al. (1983) demonstrated that the Rydberg-valence homogeneous electronic interaction is the dominant perturbation in singlet ungerade states, such as the $c_4'^1\Sigma_u^+$ state. Accordingly, we have considered the interaction between the $c_4'^1\Sigma_u^+$Rydberg and $b'^1\Sigma_u^+$ valence states in our model. The associated diabatic potential energy curves calculated with the RKR approach are shown in Figure 1. Given that the Rydberg-valence interaction causes every vibrational level to be homogeneously perturbed by several of its neighbors, in our calculations, we have taken into account the coupling of $c_4'^1\Sigma_u^+$ (6) and its nearby levels: $b'(18)^1\Sigma_u^+$, $b'(19)^1\Sigma_u^+$, $b'(20)^1\Sigma_u^+$, and $b'(21)^1\Sigma_u^+$. The eigenvector components for the five interacting diabatic states are obtained by diagonalizing the 5×5 symmetric Hamiltonian matrix for each J value. In a previous study (Velasco & Lavín 2020) involving the $c_4'^1\Sigma_u^+$ (4) state, we used the expression given by Kovács (p.207) for singlet states to determine the off-diagonal coupling parameters. This procedure is not possible for the $c_4'^1\Sigma_u^+$ (6) state because of the limited number of rotational levels observed. According to Carroll & Hagim (1988), the

Table 1
Eigenvector Components for the $c_4'^1\Sigma_u^+$ (6) Rovibronic States of N_2

J'	C_k^2 $c_4'^1\Sigma_u^+$ (6) character	C_k^2 $b'^1\Sigma_u^+$ (20) character	C_k^2 $b'^1\Sigma_u^+$ (21) character	C_k^2 $b'^1\Sigma_u^+$ (18) character	C_k^2 $b'^1\Sigma_u^+$ (19) character
0	0.911	0.031	0.022	0.026	0.010
1	0.911	0.031	0.022	0.026	0.010
2	0.911	0.031	0.022	0.025	0.010
3	0.911	0.032	0.022	0.025	0.009
4	0.911	0.033	0.023	0.025	0.008
5	0.911	0.034	0.023	0.024	0.008
6	0.910	0.036	0.023	0.024	0.007
7	0.909	0.038	0.024	0.023	0.006
8	0.907	0.041	0.024	0.023	0.005
9	0.904	0.044	0.025	0.022	0.005
10	0.901	0.048	0.026	0.021	0.004
11	0.896	0.054	0.027	0.021	0.003
12	0.889	0.061	0.027	0.020	0.003
13	0.880	0.070	0.028	0.019	0.003
14	0.867	0.083	0.029	0.018	0.002
15	0.850	0.101	0.030	0.017	0.002
16	0.824	0.127	0.031	0.016	0.002
17	0.785	0.167	0.032	0.015	0.001
18	0.727	0.227	0.031	0.014	0.001
19	0.639	0.319	0.029	0.012	0.001
20	0.516	0.449	0.025	0.009	0.001

off-diagonal elements may be written as:

$$H_{vv'}^{ee'} = H^{ee'} S_{vv'}^{ee'} \quad (5)$$

where $H^{ee'}$, a constant for two given states, is the electronic interaction parameter and $S_{vv'}^{ee'}$ is the vibrational overlap integral. In our mentioned work (Velasco & Lavín 2020), a value of 1100 cm^{-1} was estimated for the interaction parameter between the $c_4'^1\Sigma_u^+$ and $b'^1\Sigma_u^+$ electronic states. This value has been adopted in the present calculations and the vibrational overlap integrals calculated from the RKR method. The diagonal elements, which are the unperturbed rotational energies of the $c_4'^1\Sigma_u^+$ and $b'^1\Sigma_u^+$ vibrational states, are obtained by fitting the eigenvalues to experimentally determined energy terms for the rotational levels of the $c_4'^1\Sigma_u^+$ (6), $b'^1\Sigma_u^+$ (18), $b'^1\Sigma_u^+$ (19), $b'^1\Sigma_u^+$ (20), and $b'^1\Sigma_u^+$ (21) states. As pointed out by Walter et al. (2000), a first assessment of the quality of the deperturbation scheme can be made by comparing the calculated rovibrational term energies to the observed values. Experimentally, term values have been reported for $J = 0$–15 of $c_4'^1\Sigma_u^+$ (6), $J = 0$–16 of $b'^1\Sigma_u^+$ (18), $J = 0$–24 of $b'^1\Sigma_u^+$ (19), $J = 0$–21 of $b'^1\Sigma_i^+$ (20), and $J = 0$–22 of $b'(21)^1\Sigma_u^+$ (Roncin et al. (1998) and Harvard–Smithsonian Center for Astrophysics). The deperturbation procedure was performed quite satisfactorily with a mean absolute deviation of less than 1.2 cm^{-1}. The eigenvector components of the c_4' $^1\Sigma_u^+$ (6) state are given in Table 1. The Rydberg-valence mixing is small at low values of J but are not negligible (91.1% of Rydberg character and 8.9% of valence character). The percentage of $b'^1\Sigma_u^+$ character, primarily $b'(20)^1\Sigma_u^+$, increases with J until it approaches 48.4 % at $J = 20$.

The transition wavenumbers, along with the perturbed absorption oscillator strengths for the lines of the R and P branches of the $c_4'^1\Sigma_u^+(v' = 6)$-$X^1\Sigma_g^+(v'' = 0$–$9)$ bands, are given in Tables 2–6. The experimental transition wavenumbers are also shown for comparative purposes. We subtracted the appropriate ground state level (Edwards et al. 1993) from each perturbed rovibronic term presently calculated to obtain line transition energies. Comparison with the observed absorption and emission line positions (CfA Molecular Data) shows a mean absolute deviation of 0.41 cm^{-1}. It should be mentioned that about half of the comparative rotational lines are blended.

In the calculations of the oscillator strengths, we have used the MQDO formalism to determine the unperturbed $c_4'^1\Sigma_u^+$-$X^1\Sigma_g^+$ transition moment. To this end, we needed the ionization energy of N_2 and the electronic energy of the Rydberg state $c_4'^1\Sigma_u^+$ as input. For the ionization energy, we have used the experimental value obtained by Huber & Jungen (1990), and for the Rydberg electronic energy, the experimental value reported by Huber & Herzberg (1979). The MQDO vertical electronic transition moment for $c_4'^1\Sigma_u^+$-$X^1\Sigma_g^+$ is −0.6568 au. Stahel et al. (1983) reported a value of −0.5946 au, derived by fitting the vibronic band strength, calculated based on electronically coupled diabatic states, to the experimental band strength. A reasonable agreement exists between both values. For the $b'^1\Sigma_u^+$-$X^1\Sigma_g^+$ transition moment, we have used that reported by Spelsberg & Meyer (2001).

As can be observed from Tables 2–6, our calculations predict that the most intense absorption bands of the $c_4'^1\Sigma_u^+$ (6)-$X^1\Sigma_g^+(v'')$ progression are the $c_4'^1\Sigma_u^+$ (6)-$X^1\Sigma_g^+(5)$ and $c_4'^1\Sigma_u^+$ (6)-$X^1\Sigma_g^+(7)$ bands. The f -values of the P branch of both transitions increase up to $J \approx 15$, falling off thereafter, while the R branch values of both bands decrease with J.

In the absence of perturbations, the f-values for lines of the $c_4'^1\Sigma_u^+$ (6)-$X^1\Sigma_g^+(0)$ and $c_4'^1\Sigma_u^+$ (6)-$X^1\Sigma_g^+(1)$ bands are of the order of 10^{-9} and 10^{-7}, respectively, owing to the small vibrational overlap integral between the $c_4'^1\Sigma_u^+$ (6) state and the $X^1\Sigma_g^+(0)$ and $X^1\Sigma_g^+(1)$ states, 0.00018 and 0.0021, respectively. The increase in the oscillator strengths in these bands, and its consequent observation in the N_2 EUV spectra, is understable in terms of the valence character acquired by the $c_4'^1\Sigma_u^+$ (6) level through the perturbative interaction of the $c_4'^1\Sigma_u^+$-$b'^1\Sigma_u^+$ states. In fact, for these bands, the contribution to the rovibronic transition moment comes entirely from the $b'^1\Sigma_u^+$ states.

The perturbed oscillator strengths calculated by the combinations of Equations (1) and (3) involve either the sum or the difference of terms containing the unperturbed rovibronic transition moments. So, the homogeneous interaction can lead to constructive or destructive interference in the line f -value. Lines of both branches of the $c_4'^1\Sigma_u^+$ (6)-$X^1\Sigma_g^+(3)$ bands are very weak at low and medium J values due to destructive interference. However, a noticeable increase in line f-values is shown at high J values because the transition moment is dominated by $b'^1\Sigma_u^+$, mainly $b'^1\Sigma_u^+$ (20). Destructive interference is also found in the R and P branches of the $c_4'^1\Sigma_u^+$ (6)-$X^1\Sigma_g^+$ (6) band. In contrast, the analysis of the $c_4'^1\Sigma_u^+$ (6) and $b'^1\Sigma_u^+$ contributions to the transition moments for the $c_4'^1\Sigma_u^+$ (6)-$X^1\Sigma_g^+$ (4) and $c_4'^1\Sigma_u^+$ (6)-$X^1\Sigma_g^+(8)$ bands reveals that the interference is constructive for these bands. For example, oscillator strengths for lines of the P and R branches of the $c_4'^1\Sigma_u^+$ (6)-$X^1\Sigma_g^+$ (4) band are at twice the unperturbed values.

No comparative data, to our knowledge, have been reported in the literature for the f-values of lines studied here, despite the fact that the line positions of the bands belonging to the $c_4'^1\Sigma_u^+$ (6)-$X^1\Sigma_g^+(v'')$ progression have been known for many years. However, band f-values have been reported for the $c_4'^1\Sigma_u^+$

Table 2
Transition Wavenumbers (in cm^{-1}) and Absorption Oscillator Strengths for the *R* and *P* Branches of the $c_4'^1\Sigma_u^+$ (6)-$X^1\Sigma_g^+$(v″=0,1) Bands of N_2

	$c_4'^1\Sigma_u^+$ (6)-$X^1\Sigma_g^+$(0)						$c_4'^1\Sigma_u^+$ (6)-$X^1\Sigma_g^+$(1)					
	R branch			*P* branch			*R* branch			*P* branch		
J″	ν^a	ν^b	f^a	ν^a	ν^b	f^a	ν^a	ν^b	f^a	ν^a	ν^b	f^a
0	116810.77	116810.2	0.0089				114480.86	114480.54	0.0056			
1	116813.81	116813.3	0.0059	116803.27	116802.7	0.0030	114483.93	114483.66	0.0037	114473.39	114472.90	0.0019
2	116816.40	116816.0	0.0053	116798.83	116798.3	0.0036	114486.60	114486.44B	0.0034	114469.03	114468.61	0.0022
3	116818.54	116818.1	0.0050	116793.92	116793.5	0.0038	114488.83	114488.81	0.0032	114464.21	114463.78	0.0024
4	116820.22	116819.9	0.0048	116788.55	116788.1	0.0039	114490.66	114490.67B	0.0031	114458.99	114458.68	0.0025
5	116821.46	116821.1	0.0047	116782.73	116782.4	0.0040	114492.07	114490.67B	0.0031	114453.34	114453.09B	0.0025
6	116822.27	116822.0	0.0046	116776.46	116776.2	0.0040	114493.09	114493.13B	0.0031	114447.28	114447.10	0.0026
7	116822.64	116822.0B	0.0046	116769.74	116769.5	0.0040	114493.70	114493.13B	0.0031	114440.80	114440.63	0.0026
8	116822.58	116823.2	0.0046	116762.60	116762.3	0.0041	114493.92		0.0031	114433.94	114433.75	0.0027
9	116822.09	116822.0B	0.0046	116755.02	116754.4	0.0041	114493.75		0.0032	114426.68	114425.62B	0.0027
10	116821.15	116820.9B	0.0047	116747.02	116747.7	0.0041	114493.15		0.0033	114419.02	114419.79	0.0028
11	116819.73	116820.3B	0.0048	116738.59	116738.6	0.0042	114492.11		0.0034	114410.97	114411.03	0.0029
12	116817.78	116818.1B	0.0050	116729.70	116729.2	0.0043	114490.57		0.0036	114402.49	114402.14	0.0030
13	116815.23	116815.9B	0.0053	116720.34	116720.7	0.0044	114488.48		0.0038	114393.59	114394.02	0.0031
14	116811.92	116813.2B	0.0056	116710.45	116710.8	0.0046	114485.66		0.0042	114384.19	114383.99	0.0033
15	116807.61		0.0062	116699.97	116700.4	0.0049	114481.87		0.0047	114374.23	114373.98	0.0036
16	116801.89		0.0069	116688.74	116689.8	0.0053	114476.70		0.0054	114363.55		0.0039
17	116794.03		0.0080	116676.51		0.0058	114469.43		0.0063	114351.91		0.0044
18	116782.81		0.0094	116662.87		0.0065	114458.84		0.0075	114338.90		0.0050
19	116766.40		0.0110	116647.09		0.0075	114443.09		0.0089	114323.78		0.0059
20				116627.96		0.0089				114305.35		0.0071

Notes.
[a] This work.
[b] CfA Molecular Data (values with B are blended lines).

(6)-$X^1\Sigma_g^+$(0) band from high-resolution absorption spectra (Huber et al. 2009; Heays 2010). Therefore, to assess the accuracy of the present results, we have calculated the oscillator strength for this band. To do so, we first calculated the integrated absorption cross-sections for both the *P* and *R* lines of the $c_4'^1\Sigma_u^+$(4)-$X^1\Sigma_g^+$(0) band through the expression given by Nicholls (1969):

$$\int_{J'-J''}(\nu)d\nu = \frac{\pi e^2}{mc^2}\frac{N_{J''}}{N_{\rm tot}}f_{v'J',v''J''}, \quad (6)$$

where ν is the frequency in cm^{-1} and $N_{J''/N_{\rm tot}}$ is the relative population of the rotational level J'' of the lower electronic state. We assumed a Boltzmann distribution for the rotational population calculations. The results were obtained at a temperature of 300 K.

We then derived the band *f*-value, $f_{v'v''}$, by adding up the integrated absorption cross-section contributions from all the rotational lines and, finally, the resulting value was converted into band oscillator strength by using the equation (Morton & Noreau 1994):

$$f_{v'v''} = \frac{mc^2}{\pi e^2}\int(\nu)d\nu. \quad (7)$$

Our calculated *f*-value for the $c_4'^1\Sigma_u^+$(6)-$X^1\Sigma_g^+$(0) band is 0.0096, which lies within the error limits of the rotationless band *f*-value of 0.008 ± 0.002 obtained by Heays (2010) from high-resolution integrated cross-sections of individual rotational lines at a temperature of 300 K. Huber et al. (2009) derived *f*-values for several bands of N_2 from band-integrated optical depth measurements carried out on cold supersonic jet expansions. For the $c_4'^1\Sigma_u^+$(6)-$X^1\Sigma_g^+$(0) band, they reported a value of 0.0117 ± 0.0010 which shows a reasonable agreement with our result. It should be noted that Huber et al. (2009) claimed that the band *f* -values very likely depend on temperature due to the perturbations. No comparison with other works can be made, since there are no experimental or theoretical band *f*-values for the remaining bands studied in this work. Nevertheless, it should be mentioned that the bands in the $c_4'^1\Sigma_u^+$ (6) progression were identified in discharge measurements at high spectral resolution by Roncin et al. (1987). These researchers noted that the $c_4'^1\Sigma_u^+$ (6)-$X^1\Sigma_g^+$(1) and $c_4'^1\Sigma_u^+$ (6)-$X^1\Sigma_g^+$(2) bands are weak, the $c_4'^1\Sigma_u^+$ (6)-$X^1\Sigma_g^+$(3) band is very weak, the $c_4'^1\Sigma_u^+$ (6)-$X^1\Sigma_g^+$ (4) and $c_4'^1\Sigma_u^+$ (6)-$X^1\Sigma_g^+$(8) bands are strong, and the $c_4'^1\Sigma_u^+$ (6)-$X^1\Sigma_g^+$(5) and $c_4'^1\Sigma_u^+$ (6)-$X^1\Sigma_g^+$(7) bands are very strong. Our results display a similar behavior as can be seen from Tables 2–6.

We have also calculated the radiative lifetimes ($\tau_{v'J'}$) of rotational levels of the $c_4'^1\Sigma_u^+$ (6) state using the expression given by Larsson (1983):

$$\tau_{v'J'} = \frac{1}{\sum_{v''J''}A_{v'J',v''J''}}, \quad (8)$$

where $A_{v'J',v''J''}$ is the transition probability for a spontaneous radiative transition from an excited rovibronic state (v', J') to a state (v'', J''), and it is related to the absorption line oscillator strength through the expression:

$$A_{v'J',v''J''} = 0.667\nu^2_{v'J',v''J''}\frac{2J''+1}{2J'+1}f_{v'J',v''J''}, \quad (9)$$

Table 3
Transition Wavenumbers (in cm^{-1}) and Absorption Oscillator Strengths for the *R* and *P* Branches of the $c'^1_4\Sigma^+_u$ (6)-$X^1\Sigma^+_g$(v″=2,3) Bands of N_2

	$c'^1_4\Sigma^+_u$ (6)-$X^1\Sigma^+_g$(2)						$c'^1_4\Sigma^+_u$ (6)-$X^1\Sigma^+_g$(3)					
	R branch			*P* branch			*R* branch			*P* branch		
J″	ν^a	ν^b	f^a	ν^a	ν^b	f^a	ν^a	ν^b	f^a	ν^a	ν^b	f^a
0	112179.62	112179.27	0.0012				109907.07	109906.27B	0.0002			
1	112182.73	112182.39	0.0008	112172.19		0.0004	109910.22	109909.71B	0.0001	109899.68		0.0001
2	112185.46	112185.24	0.0007	112167.89	112167.48	0.0005	109913.02	109912.54	0.0001	109895.45		0.0001
3	112187.80	112187.75	0.0006	112163.18	112162.75B	0.0005	109915.47		0.0001	109890.85	109890.98B	0.0001
4	112189.76	112189.60	0.0006	112158.09	112157.79	0.0005	109917.57	109917.12	0.0001	109885.90	109885.36B	0.0001
5	112191.35		0.0006	112152.62	112152.39	0.0005	109919.33		0.0001	109880.60		0.0001
6	112192.58	112192.93B	0.0006	112146.77	112146.57	0.0005	109920.77	109920.98	0.0001	109874.96	109874.95B	0.0001
7	112193.44	112192.93B	0.0006	112140.54	112140.38	0.0005	109921.87		0.0001	109868.97		0.0001
8	112193.93		0.0005	112133.95	112133.76	0.0005	109922.65		0.0001	109862.67	109862.57B	0.0001
9	112194.07		0.0005	112127.00	112126.45	0.0005	109923.11		0.0002	109856.04		0.0001
10	112193.82		0.0005	112119.69	112120.50	0.0005	109923.20		0.0002	109849.07	109849.62	0.0001
11	112193.17		0.0005	112112.03	112112.17	0.0005	109922.93		0.0002	109841.79	109842.82B	0.0001
12	112192.05		0.0005	112103.97	112103.64	0.0005	109922.24		0.0002	109834.16		0.0002
13	112190.41		0.0006	112095.52	112096.02	0.0005	109921.05		0.0003	109826.16	109826.51B	0.0002
14	112188.08		0.0006	112086.61	112086.58	0.0005	109919.21		0.0004	109817.74		0.0002
15	112184.81		0.0007	112077.17	112076.93	0.0005	109916.47		0.0005	109808.83	109810.00B	0.0003
16	112180.20		0.0007	112067.05		0.0006	109912.42		0.0006	109799.27		0.0003
17	112173.53		0.0008	112056.01		0.0006	109906.34		0.0009	109788.82		0.0004
18	112163.56		0.0010	112043.62		0.0007	109897.00		0.0013	109777.06		0.0006
19	112148.47		0.0012	112029.16		0.0008	109882.58		0.0019	109763.27		0.0009
20				112011.43		0.0010				109746.23		0.0012

Notes.
[a] This work.
[b] CfA Molecular Data (values with B are blended lines).

Table 4
Transition Wavenumbers (in cm^{-1}) and Absorption Oscillator Strengths for the *R* and *P* Branches of the $c'^1_4\Sigma^+_u$ (6)-$X^1\Sigma^+_g$(v″=4,5) Bands of N_2

	$c'^1_4\Sigma^+_u$ (6)-$X^1\Sigma^+_g$ (4)						$c'^1_4\Sigma^+_u$ (6)-$X^1\Sigma^+_g$(5)					
	R branch			*P* branch			*R* branch			*P* branch		
J″	ν^a	ν^b	f^a	ν^a	ν^a	f^a	ν^a	ν^b	f^a	ν^a	ν^b	f^a
0	107663.27	107662.80	0.0195				105448.23	105447.82	0.0456			
1	107666.45	107666.09	0.0130	107655.91		0.0065	105451.44	105451.63B	0.0304	105440.90	105440.41B	0.0152
2	107669.32	107669.16	0.0117	107651.75		0.0078	105454.39	105454.08B	0.0274	105436.82	105436.38	0.0182
3	107671.87	107671.60	0.0111	107647.25	107646.73B	0.0084	105457.04	105456.57	0.0261	105432.42	105431.78B	0.0195
4	107674.11	107673.89B	0.0107	107642.44	107641.96	0.0086	105459.43	105459.19	0.0255	105427.76	105427.43B	0.0203
5	107676.05	107675.91	0.0105	107637.32	107637.14	0.0088	105461.54	105461.38	0.0251	105422.81	105422.54	0.0208
6	107677.70	107677.55	0.0103	107631.89	107631.61	0.0089	105463.40	105463.23	0.0248	105417.59	105417.38	0.0212
7	107679.05	107678.27	0.0102	107626.15	107625.93	0.0090	105465.00	105464.51B	0.0247	105412.10	105411.88	0.0214
8	107680.11		0.0101	107620.13		0.0090	105466.34	105467.38B	0.0246	105406.36	105406.13B	0.0217
9	107680.88		0.0100	107613.81	107613.12	0.0090	105467.43	105467.38B	0.0245	105400.36	105399.77	0.0219
10	107681.33		0.0100	107607.20		0.0091	105468.23	105467.38B	0.0244	105394.10	105394.85	0.0221
11	107681.44		0.0099	107600.30	107600.00B	0.0091	105468.73	105469.05	0.0244	105387.59	105387.63B	0.0222
12	107681.17		0.0099	107593.09		0.0091	105468.88		0.0244	105380.80	105380.42	0.0224
13	107680.44		0.0100	107585.55	107585.91	0.0092	105468.61		0.0244	105373.72	105374.13	0.0225
14	107679.09		0.0100	107577.62	107577.65	0.0092	105467.75		0.0243	105366.28	105366.14	0.0226
15	107676.87		0.0101	107569.23		0.0093	105466.07		0.0241	105358.43	105359.46B	0.0227
16	107673.39		0.0102	107560.24		0.0094	105463.14		0.0237	105349.99	105350.94B	0.0227
17	107667.90		0.0103	107550.38		0.0095	105458.26		0.0229	105340.74		0.0226
18	107659.20		0.0102	107539.26		0.0096	105450.18		0.0215	105330.24		0.0224
19	107645.44		0.0098	107526.13		0.0097	105437.10		0.0190	105317.79		0.0217
20				107509.80		0.0097				105302.16		0.0203

Notes.
[a] This work.
[b] CfA Molecular Data (values with B are blended lines).

Table 5
Transition Wavenumbers (in cm^{-1}) and Absorption Oscillator Strengths for the *R* and *P* Branches of the $c'^1_4\Sigma^+_u$ (6)-$X^1\Sigma^+_g$($v'' = 6, 7$) Bands of N_2

	$c'^1_4\Sigma^+_u$ (6)-$X^1\Sigma^+_g$ (6)						$c'^1_4\Sigma^+_u$ (6)-$X^1\Sigma^+_g$(7)					
	R branch			*P* branch			*R* branch			*P* branch		
J''	ν[a]	ν[b]	f[a]	ν[a]	ν[b]	f[a]	ν[a]	ν[b]	f[a]	ν[a]	ν[b]	f[a]
0	103262.01	103261.49B	0.0067				101104.65	101104.29B	0.0403			
1	103265.26	103265.47B	0.0045	103254.72	103254.92B	0.0022	101107.94	101107.57B	0.0269	101097.40	101097.11B	0.0134
2	103268.27	103267.68B	0.0041	103250.70	103250.14B	0.0027	101111.02	101110.75	0.0243	101093.45	101092.98	0.0161
3	103271.03	103270.68	0.0039	103246.41	103245.23B	0.0029	101113.89	101113.69	0.0232	101089.27	101088.93B	0.0173
4	103273.56	103273.53B	0.0038	103241.89	103241.89B	0.0030	101116.56	101116.44	0.0226	101084.89	101084.59B	0.0180
5	103275.85	103275.17B	0.0037	103237.12	103236.73	0.0031	101119.02	101118.91	0.0222	101080.29	101080.10B	0.0184
6	103277.92	103277.48B	0.0037	103232.11	103232.17B	0.0031	101121.31	101121.16B	0.0220	101075.50	101075.30	0.0188
7	103279.77	103279.23B	0.0036	103226.87	103226.50	0.0032	101123.40	101122.86B	0.0219	101070.50	101070.31B	0.0190
8	103281.39	103282.21B	0.0035	103221.41	103221.01B	0.0032	101125.31	101126.19B	0.0217	101065.33	101065.12	0.0192
9	103282.80	103282.21B	0.0035	103215.73	103215.28	0.0032	101127.03	101127.06B	0.0216	101059.96	101059.52B	0.0194
10	103283.95	103283.12B	0.0034	103209.82	103210.44B	0.0032	101128.54	101128.06	0.0215	101054.41	101055.21B	0.0195
11	103284.84	103285.21B	0.0033	103203.70	103203.92B	0.0031	101129.83	101130.31	0.0214	101048.69	101048.88B	0.0196
12	103285.42		0.0031	103197.34	103196.97	0.0031	101130.83		0.0212	101042.75	101042.39B	0.0197
13	103285.60		0.0029	103190.71	103191.30B	0.0030	101131.47		0.0209	101036.58	101037.06B	0.0197
14	103285.24		0.0026	103183.77	103183.69	0.0029	101131.61		0.0205	101030.14	101030.17B	0.0196
15	103284.09		0.0023	103176.45	103177.03B	0.0027	101130.99		0.0200	101023.35		0.0195
16	103281.73		0.0019	103168.58	103168.55B	0.0025	101129.20		0.0191	101016.05	101016.85B	0.0192
17	103277.44		0.0013	103159.92		0.0022	101125.52		0.0177	101008.00		0.0188
18	103270.01		0.0007	103150.07		0.0018	101118.72		0.0156	100998.78		0.0180
19	103257.60		0.0002	103138.29		0.0013	101106.99		0.0126	100987.68		0.0168
20				103123.37		0.0007				100973.46		0.0148

Notes.
[a] This work.
[b] CfA Molecular Data (values with B are blended lines).

Table 6
Transition Wavenumbers (in cm^{-1}) and Absorption Oscillator Strengths for the *R* and *P* Branches of the $c'^1_4\Sigma^+_u$ (6)-$X^1\Sigma^+_g$(v″=8,9) Bands of N_2

	$c'^1_4\Sigma^+_u$ (6)-$X^1\Sigma^+_g$(8)						$c'^1_4\Sigma^+_u$ (6)-$X^1\Sigma^+_g$(9)					
	R branch			*P* branch			*R* branch			*P* branch		
J″	ν^a	ν^b	f^a	ν^a	ν^b	f^a	ν^a	ν^b	f^a	ν^a	ν^b	f^a
0	98976.21	98975.41B	0.0213				96876.73	96876.32	0.0040			
1	98979.53	98979.00	0.0142	98968.99	98968.44B	0.0071	96880.09	96879.81	0.0027	96869.55	96869.68B	0.0014
2	98982.68	98982.17B	0.0128	98965.11	98964.49B	0.0085	96883.32	96883.00B	0.0024	96865.75	96865.22B	0.0016
3	98985.66	98985.25B	0.0122	98961.04	98960.58	0.0091	96886.40	96886.06B	0.0023	96861.78	96861.23	0.0017
4	98988.47	98987.96B	0.0119	98956.80	98956.23B	0.0095	96889.36	96889.04	0.0022	96857.69	96857.11B	0.0018
5	98991.11	98990.79	0.0117	98952.38	98951.94B	0.0097	96892.18	96891.92	0.0021	96853.45	96853.29B	0.0018
6	98993.61	98993.24	0.0115	98947.80	98947.49B	0.0099	96894.89	96894.64B	0.0021	96849.08	96848.82	0.0018
7	98995.96	98995.25	0.0115	98943.06	98942.75B	0.0100	96897.49	96896.71B	0.0020	96844.59	96844.25	0.0018
8	98998.15	98998.93B	0.0114	98938.17	98937.75	0.0101	96899.96	96900.67	0.0020	96839.98	96839.69B	0.0018
9	99000.19	98999.99B	0.0114	98933.12	98932.38B	0.0102	96902.33	96902.26	0.0020	96835.26	96834.6	0.0018
10	99002.06	99000.89B	0.0115	98927.93	98928.52	0.0103	96904.55	96903.99B	0.0020	96830.42	96831.08	0.0018
11	99003.73	99003.97	0.0115	98922.59	98922.52B	0.0104	96906.62	96906.88B	0.0020	96825.48	96825.26B	0.0018
12	99005.16		0.0116	98917.08	98916.53	0.0105	96908.48		0.0020	96820.40	96819.35B	0.0018
13	99006.27		0.0118	98911.38	98911.66	0.0106	96910.05		0.0020	96815.16		0.0018
14	99006.91		0.0119	98905.44		0.0108	96911.19		0.0020	96809.72		0.0018
15	99006.82		0.0121	98899.18		0.0110	96911.64		0.0020	96804.00		0.0018
16	99005.60		0.0123	98892.45		0.0112	96910.99		0.0021	96797.84		0.0019
17	99002.52		0.0124	98885.00		0.0114	96908.52		0.0021	96791.00		0.0019
18	98996.37		0.0124	98876.43		0.0116	96903.01		0.0022	96783.07		0.0020
19	98985.31		0.0119	98866.00		0.0118	96892.63		0.0022	96773.32		0.0020
20				98852.50		0.0117				96760.54		0.0021

Notes.
[a] This work.
[b] CfA Molecular Data (values with B are blended lines).

where $\nu_{v'J',v''J''}$ is the wavenumber for the transition in cm^{-1} and $A_{v'J',v''J''}$ is expressed in s^{-1}.

In the calculation of the lifetime, we have considered transitions from rotational levels of the $c_4'^1\Sigma^+_u$ (6) state to the appropriate rotational levels of the $X^1\Sigma^+_g$ and $a''^1\Sigma^+_g$ states since transitions to the latter are dipole allowed. The electronic transition moment for the $c_4'^1\Sigma_u^+$-$a''^1\Sigma^+_g$ transition calculated with the MQDO formalism is -3.0 au. No comparative data have been found in the literature. Although the $c_4'^1\Sigma_u^+$-$a''^1\Sigma^+_g$ electronic transition moment is large when compared to that of $c_4'^1\Sigma_u^+$-$X^1\Sigma^+_g$, the contribution of the emission to the $a''^1\Sigma^+_g$ states to the global transition probability turns out to be less than 0.2% because the frequencies of the $c_4'^1\Sigma_u^+$(6)-$a''^1\Sigma^+_g$(v″) transitions are very small. In fact, the $c_4'^1\Sigma_u^+$-$a''^1\Sigma^+_g$ and $c_4'^1\Sigma_u^+$-$X^1\Sigma^+_g$systems fall into the near-infrared and the EUV, respectively.

Radiative lifetimes for the individual rotational levels ($J = 0$–20) of the $c_4'^1\Sigma^+_u$ (6) state are given in Table 7. Our model predicts a small rotational dependence on the radiative lifetime of the $c_4'^1\Sigma^+_u$ (6) state for $J \leqslant 19$. Thereby, radiative lifetimes remain constant with a value of 0.89 ns over the $J = 0$–10 range and then smoothly decrease until 0.84 ns as the interaction $c_4'^1\Sigma^+_u$-$b'^1\Sigma^+_u$ increases. These values are somewhat larger than the only value reported, 0.61 ± 0.13 ns, which is a rotationally averaged fluorescence lifetime of the $c_4'^1\Sigma^+_u$ (6) state obtained by Moise et al. (2011). Taking into account the fact that predissociation and spontaneous emission are the two primary decay mechanisms for the excited states of N_2 (Liu et al. 2009), the shorter experimental lifetime, compared to our values of radiative lifetimes, could be indicative of the predissociation of the $c_4'^1\Sigma^+_u$ (6) state through its coupling with the $b'^1\Sigma^+_u$ states which in turn are predissociated by continuum states (Helm et al. 1993).

Table 7
Radiative Lifetimes (in ns) as a Function of J, for the $c'^1_4\Sigma^+_u$ (6) State of N_2

J′	τ
0	0.89
1	0.89
2	0.89
3	0.89
4	0.89
5	0.89
6	0.89
7	0.89
8	0.89
9	0.89
10	0.89
11	0.88
12	0.88
13	0.87
14	0.87
15	0.86
16	0.85
17	0.84
18	0.84
19	0.84

To summarize, in this study, we have calculated transition energies and oscillator strengths for the rotational lines of the $c_4'^1\Sigma^+_u$ (6)-$X^1\Sigma^+_g$(v″ = 0–9) bands in molecular nitrogen, and the radiative lifetimes of rotational levels of the $c_4'^1\Sigma^+_u$ (6) state. In the calculations, we have used a model that includes the perturbations between the $c_4'^1\Sigma^+_u$ (6) Rydberg state and $b'^1\Sigma^+_u$

valence states. The comparison between *R*- and *P*-line positions presently calculated and experimental results, when available, suggest that the procedure used properly takes into account the valence-Rydberg perturbation. To the best of our knowledge, the line *f*-values for the bands of the $c_4'^1\Sigma_u^+$ (6)-$X^1\Sigma_g^+(v'')$ progression and radiative lifetimes at the rotational level are reported here for the first time. As mentioned, several of these bands have been observed in the airglow spectra from Titan. From their spectral analysis of Cassini UVIS observations, Stevens et al. (2011) found that the N_2 $c_4'^1\Sigma_u^+(3, 4, 6)$ progressions are blended and considered all three of these progressions as one spectral component in their airglow radiance model. We hope that the new data reported here may aid to identify the contribution from each fine structure feature in the mentioned blended progressions, thus leading to understanding of the EUV spectra of atmospheres containing molecular nitrogen.

This work has been supported by the Junta de Castilla y León (UCI 139, Grant VA244P20) and the Ministerio de Ciencia e Innovación (PID2019-111396GB-I00).

ORCID iDs

A. M. Velasco https://orcid.org/0000-0003-3835-6873
J. L. Alonso https://orcid.org/0000-0002-3146-8250
P. Redondo https://orcid.org/0000-0001-7876-4818
C. Lavín https://orcid.org/0000-0002-8104-2805

References

Ajello, J. M., James, G. K., & Cioccay, M. 1998, JPhB, 31, 2437
Ajello, J. M., James, G. K., Franklin, B. O., & Shemansky, D. E. 1989, PhRvA, 40, 3524
Ajello, J. M., Stevens, M. H., Stewart, I., et al. 2007, GeoRL, 34, L24204
Carroll, P. K., & Hagim, K. I. 1988, PhyS, 37, 682
Center for Astrophysics Molecular Data, https://lweb.cfa.harvard.edu/amp/ampdata/cfamols.html#toN2
Chan, W. F., Cooper, G., Sodhi, R. N. S., & Brion, C. E. 1993, CP, 170, 81
Edwards, S., Roncin, J. Y., Launay, F., & Rostas, F. 1993, JMoSp, 162, 257
Feldman, P. D., Sahnow, D. J., Kruk, J. W., Murphy, E. M., & Moos, H. W. 2001, JGR, 106, 8119
Harvard-Smithsonian Center for Astrophysics, https://lweb.cfa.harvard.edu/amp/ampdata/N2ARCHIVE/n2term.html
Heays, A. N. 2010, PhDT, The Australian National University, p.100
Heays, A. N., Ajello, J. M., Aguilar, A., Lewis, B. R., & Gibson, S. T. 2014, ApJS, 211, 28
Helm, H., Hazell, I., & Bjerre, N. 1993, PhRvA, 48, 2762
Huber, K. P., Chan, M.-C., Stark, G., Ito, K., & Matsui, T. 2009, JChPh, 131, 084301
Huber, K. P., & Herzberg, G. 1979, Molecular Spectra and Molecular Structure. IV. Constants of Diatomic Molecules (New York: Van Nostrand Rehinhold)
Huber, K. P., & Jungen, Ch. 1990, JChPh, 92, 850
Klein, O. 1932, ZPhy, 76, 226
Kovács, I. 1969, Rotational Structure in the Spectra of Diatomic Molecules (New York: Elsevier)
Krasnopolsky, V. A., & Feldman, P. D. 2002, Icar, 160, 86
Larsson, M. 1983, A&A, 128, 291
Lavín, C., Martín, I., Mayor, E., & Velasco, A. M. 2008, MolPh, 106, 929
Lavín, C., & Velasco, A. M. 2011, ApJ, 739, 16
Lavín, C., Velasco, A. M., & Martín, I. 2010, CPL, 487, 38
Lavin, C., & Velasco, A. M. 2016, ApJ, 816, 58
Liu, X., Heays, A. N., Shemansky, D. E., et al. 2009, JGR, 114, D07304
Liu, X., Shemansky, D. E., Malone, C. P., et al. 2008, JGR, 113, A02304
Martín, I., Lavín, C., Velasco, A. M., et al. 1996, CP, 202, 307
Moise, A., Prince, K. C., & Richter, R. 2011, JPhCh, 134, 114312
Morton, D. C., & Noreau, L. 1994, ApJS, 95, 301
Nicholls, R. W. 1969, Electronic Spectra of Diatomic Molecules (New York: Elsevier)
Rees, A. L. G. 1947, PPSL, 59, 998
Roncin, J. Y., Launay, F., & Yoshino, K. 1987, P&SS, 35, 267
Roncin, J. Y., Subtil, J. L., & Launay, F. 1998, JMoSp, 188, 128
Rydberg, R. 1931, ZPh, 73, 376
Stahel, D., Leoni, M., & Dressler, K. 1983, JChPh, 79, 2541
Stark, G., Huber, K. P., Yoshino, K., et al. 2005, JChPh, 123, 214303
Stevens, M. H., Gustin, J., Ajello, J. M., et al. 2011, JGR, 116, A05304
Spelsberg, D., & Meyer, W. 2001, JChPh, 115, 6438
Velasco, A. M., & Lavin, C. 2020, ApJ, 899, 57
Walter, C. W., Cosby, P. C., & Helm, H. 2000, JChPh, 112, 4621
Whiting, R. E., & Nicholls, R. W. 1974, ApJS, 27, 1
Yoshino, K., Freeman, D. E., & Tanaka, Y. 1979, JMoSp, 76, 153
Zipf, E. C., & McLaughlin, R. W. 1978, P&SS, 26, 449